PS Mineralogical and Petrophysical Characterization of the Reservoir Facies of Doig Formation in British Columbia, Triassic of Western Canada Sedimentary Basin*

Pablo Lacerda Silva[1] and Robert Marc Bustin[1]

Search and Discovery Article #10948 (2017)**
Posted June 5, 2017

*Adapted from poster presentation given at 2017 AAPG Annual Convention & Exhibition, Houston, Texas, April 2-5, 2017

[1]Department of Earth, Ocean and Atmospheric Sciences, University of British Columbia, Vancouver, British Columbia, Canada (pablols@yahoo.com)

Abstract

The Triassic section of the Western Canada Sedimentary Basin is the richest interval within the basin in terms of volume of oil per volume of rock. The Lower and Middle Triassic Doig Formation has been historically known for the limited production from its conventional reservoirs in British Columbia (BC) and Alberta (AB). More recently, the Doig has received attention for its unconventional potential as a gas and natural gas liquids play, with estimates of total gas in-place ranging from 40 to 200 Tcf. The Doig has been informally subdivided into a lower Phosphate Zone (DPZ), and an upper siltstone interval. While the source-rock reservoir potential of the Doig is undoubtedly large, so are the uncertainties related to the spatial and stratigraphic distribution of its reservoir facies and properties. This study is an investigation of the reservoir facies of the Doig Formation in BC and characterizes its variability in porosity, pore throat size distribution, mineralogy and organic content. A grid of 15 cored wells covering its entire extent in BC, was selected. Eight reservoir facies are recognized, based on lithofacies, mineralogy by X ray diffraction (XRD), total organic carbon by Rock-Eval pyrolysis, porosity and pore size distribution by helium pycnometry and mercury intrusion, and permeability by pressure pulse-decay. In contrast to many shale reservoirs, the Doig is characterized mineralogically by a low clay content, and higher quartz and carbonate, especially dolomite. The DPZ is more clay and organic rich than the upper Doig, showing overall lower porosity and smaller average pore throat radii. In spite of these generalizations, facies stacking patterns confer a high degree of internal heterogeneity within these two major zones. Coarser and clay poor facies are characterized by median pore throat sizes three to four times larger than the finer clay rich facies. Pore throat size has a high degree of correlation with matrix permeability, which spans four orders of magnitude, from 10E-7 and 10E-4 md. Additional heterogeneity is caused by superimposing diagenetic features, such as authigenic pyrite, apatite, calcite veins and clay-smeared fractures, and may not be defined at the core or well log scales.

Mineralogical and Petrophysical Characterization of the Reservoir Facies of the Doig Formation in British Columbia, Triassic of Western Canada Sedimentary Basin

Pablo Lacerda Silva & Robert Marc Bustin

Department of Earth, Ocean and Atmospheric Sciences

Mineralogy

The Doig is primarily composed of silicates and carbonate, with minor amounts of clay (Figure 6). The main form of silica is quartz, with an average of 39%, minimum of 12% and maximum of 82%. The primary carbonate is dolomite, with an average of 26%, minimum of 4% and maximum of 72%. Other significant silicate minerals are orthoclase and albite with average values of 8% and 7%, respectively. Calcite is only locally important, with an average of 11% but reaching 62% in some samples.

The main clay mineral is illite, and the average clay content is 6%, with a maximum of 21%; some facies being completely clay-free. Some of the clay content may be due to mica, as their peaks coincide in the diffractograms of bulk mineralogy analysis. There is also a subordinate amount of chlorite. Other important minerals are apatite and pyrite, due to being present in a large number of samples, albeit in trace quantities, with maximum values of 7% and 5%, respectively.

Although the carbonate and silica content of the Doig siltstones and mudstones are highly variable, some distinctions can be made in terms of the typical mineralogy of the Doig subzones (Figure 8).

The highly cemented organic-lean massive siltstones and cross-bedded fine sandstones of the upper Doig C have no clay, and are predominantly composed of silicates, in the form of detrital quartz and cement. The mineralogy and lithology of the Doig B is much more variable, ranging from carbonate-rich massive, bioturbated or bioclastic mudstones to silica-rich wavy laminated silstones with sparse carbonate laminae. The clay content of the Doig B is highly variable and difficult to predict from a visual facies description. The Doig A mudstones have an overall higher clay content, and variable amounts of silicates and carbonate. Pyrite commonly occurs, correlating with high TOC values, which indicates an anoxic reducing depositional environment.

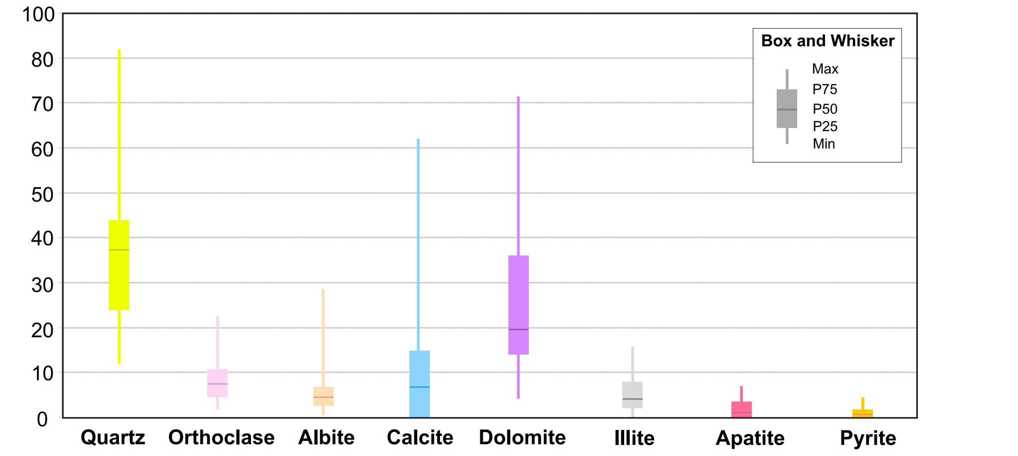

Figure 6 - Box and whisker plot of the main minerals present in the samples analyzed by XRD

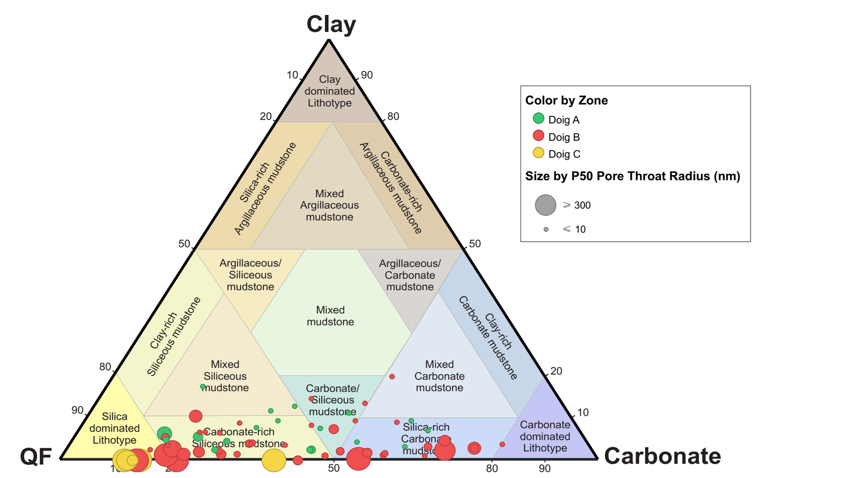

Figure 8 - Ternary diagram of the mineralogy normalized to silica, carbonate and clays, with symbols colored by Doig subzone and sized by median pore throat radius

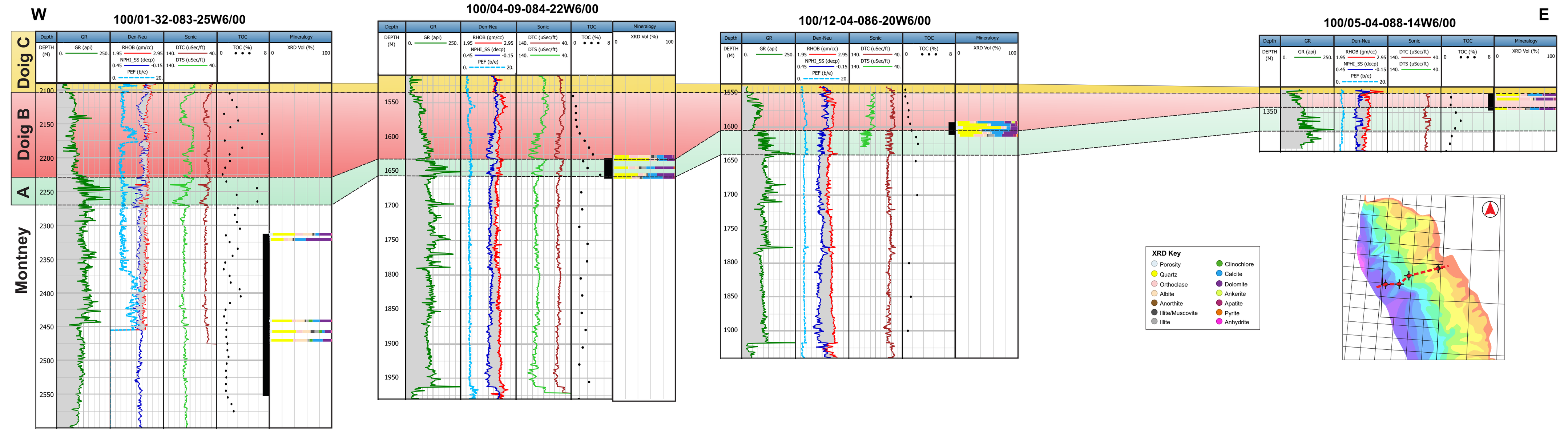

Figure 7 - West-east dip cross-section of the Doig Formation, with datum on top of Doig B, showing the correlation of the subdivision across the basin, with XRD mineralogy and TOC values

Porosity and Permeability

Porosity is highly variable, ranging from 0.6% to 16.4%, with a median of 3.3% and a P10-P90 range of 1.7% to 8.2%, as measured by He pycnometry and mercury immersion bulk density on as received samples.

The raw and the closure corrected mercury injection porosity values show a very large scatter and poor correlation with helium pycnometry, highlighting the importance of closure and compressibility corrections. The mercury injection porosity values corrected to a standard net confining stress have a very good correlation with porosity values derived from helium pycnometry (Figure 9), albeit consistently lower by roughly 20%. This difference is attributed to the lower limit of 3 nm pore sizes accessed by mercury at the pressure limit of the method, and the inaccessibility of non-interconnected pores.

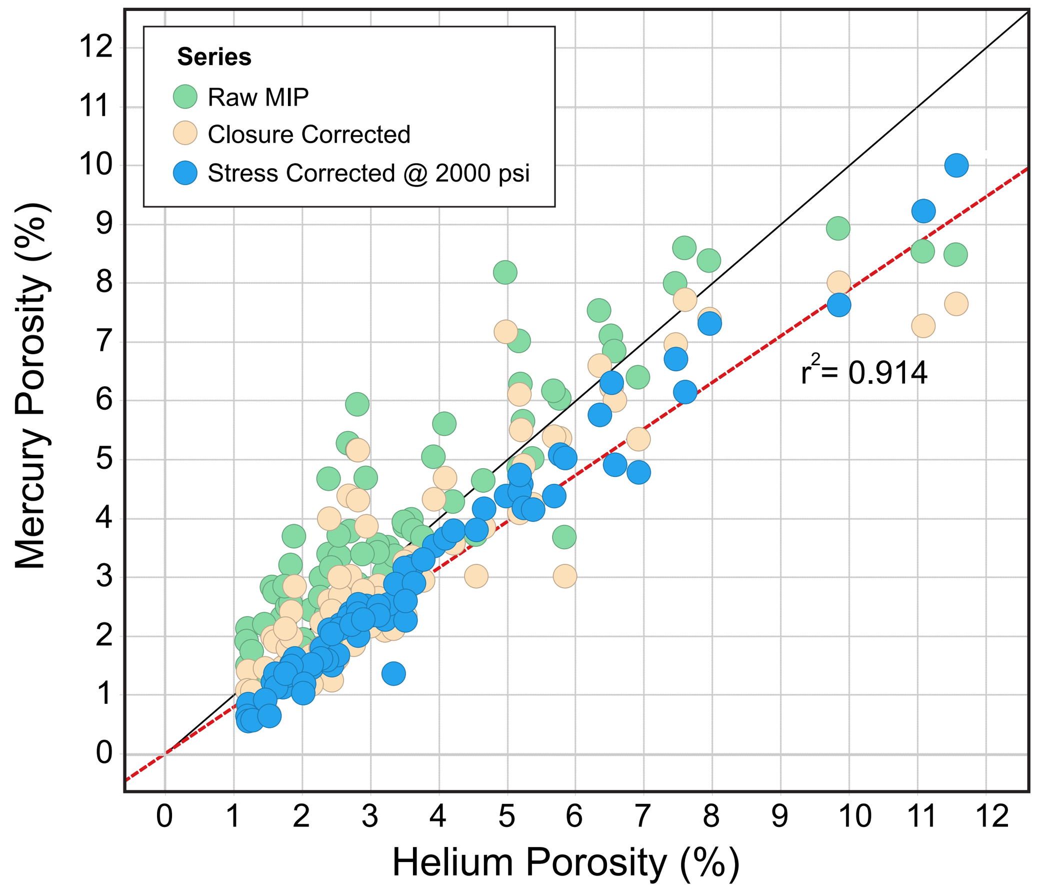

Figure 9 - Crossplot of helium pycnometry porosity and the three different steps from mercury injection porosimetry (raw, closure corrected and net confining stress corrected), highlighting the greatly improved correlation between pycnometry and mercury injection once corrected, as well as the consistently lower porosity measured by mercury injection

Matrix permeability spans four orders of magnitude, ranging from 7E-02 mD to 3.5E-05 mD at effective stresses of 2,500 psi. The permeabilities measured so far have a remarkably good correlation with porosity. The dominant factor in controlling the permeability is the widely different pore throat size distributions, which also shows a good correlation in the data acquired to date.

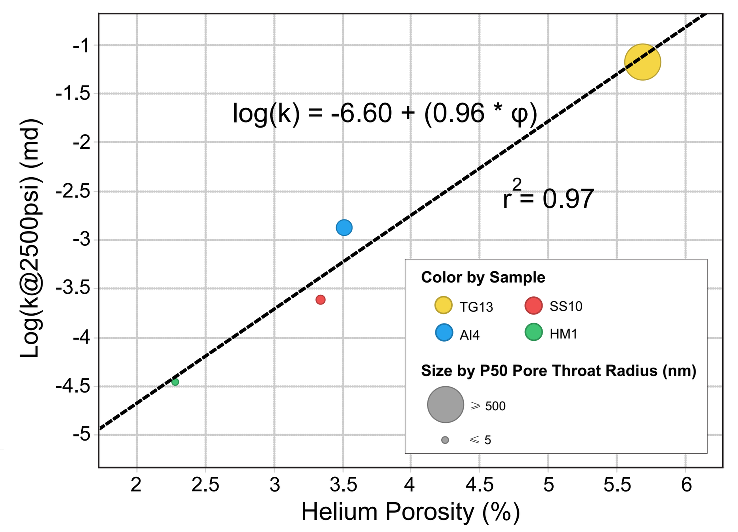

Figure 10 - Helium pycnometry porosity versus log of permeability at 2,500 psi, illustrating the very good correlation observed between these two variables, as well as the dependency on the pore throat size

The stress sensitivity of permeability obtained from measuring permeability at different effective stresses correlates well with the different reservoir facies (Figure 11). The permeability of the quartz-rich siltstones, which dominate the facies succession of Doig C, is the least stress sensitive, as the competent mineral framework is effective in preventing pore volume compression. The finer-grained samples containing 1-2% clay and 15-20% carbonate show almost one order of magnitude of permeability reduction when effective stress is increased from 1,000 to 5,000 psi. With 8% clay and 40% carbonate, the fine-grained massive mudstone facies has a permeability reduction of two orders of magnitude for the same effective stress range.

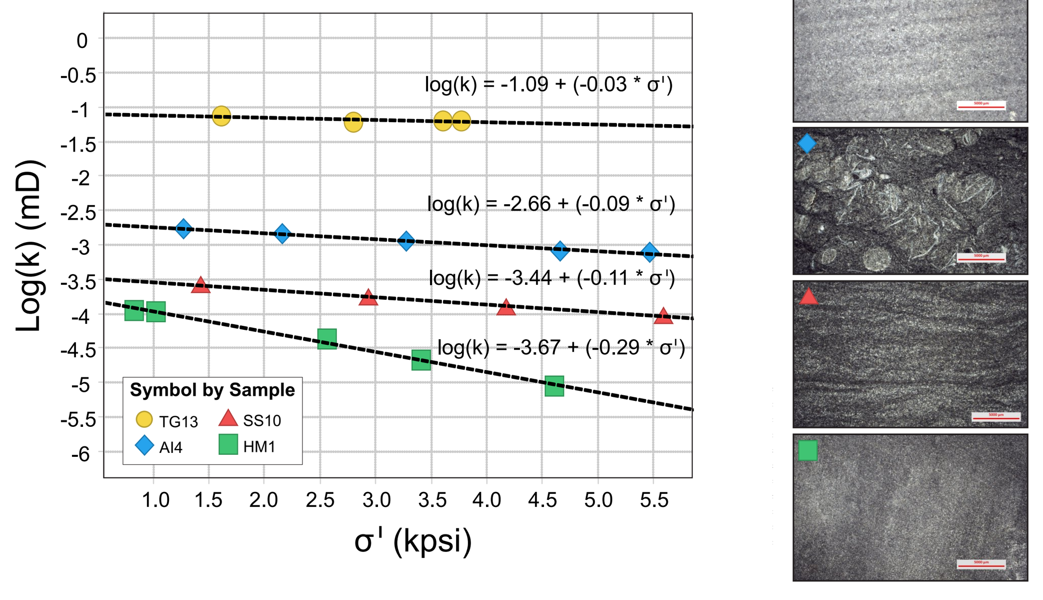

Figure 11 - Log of permeability (k) versus effective stress (σ'), showing the wide range of permeabilities, as well as the difference in permeability sensitivity to stress across reservoir facies

Pore Size Distribution and Pore Structure

The pore throat size distribution of the different reservoir facies of the Doig is highly variable, spanning three orders of magnitude (P10-P90 range). Pore throat size is partly controlled by clay content; smaller pore throats occur in samples with higher clay content, regardless of carbonate abundance.

The more organic and clay-rich mudstones of the Doig A are mostly mesoporous, having 80% of their pore volume in the 3 to 100 nm range and a median size of 10 nm. There is likely a large contribution from microporosity that is undetectable by this method, and will need low pressure gas adsorption to be quantified.

On the opposite end of the spectrum in terms of permeability and pore size distribution, is the silica-rich siltstone with a P50 pore throat radius of 490 nm and a large P10-P90 range of 50 to 1800 nm.

The difference in pore size, as well as pore type and geometry is highlighted in the SEM photomicrographs. In the silica-rich sample, the intergranular pore space is abundant and the macropores are evident. In the fine-grained carbonate mudstone, there is very little visible porosity in the form of slits in the carbonate matrix. Much of the porosity of this facies is at or below the resolution of field-emission SEM and individual micropores cannot be resolved.

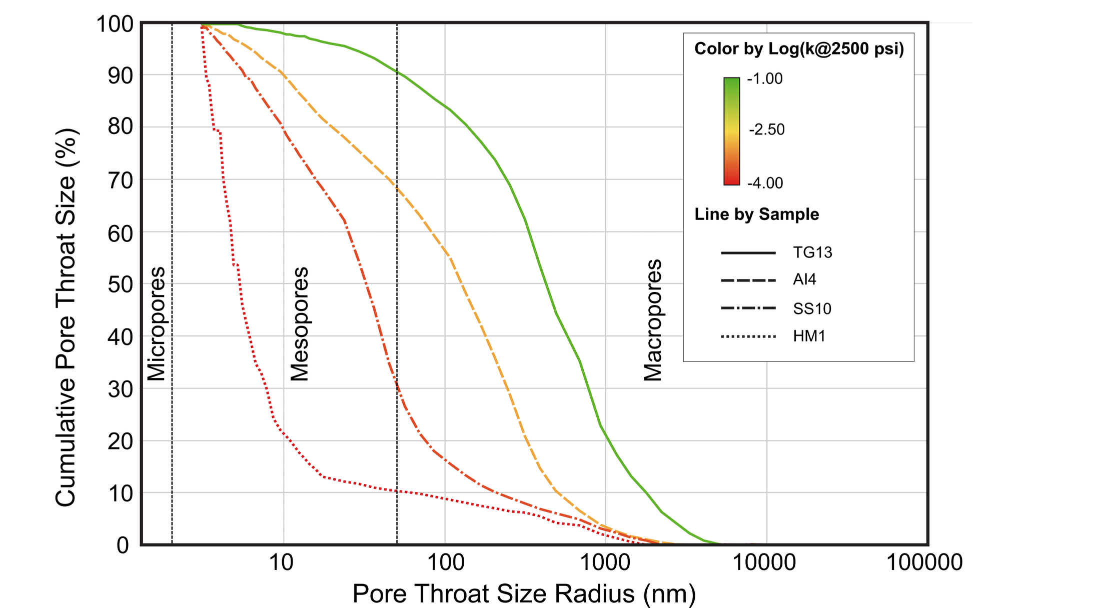

Figure 12 - Cumulative pore size distribution curves as percentage of total porosity, colored by the log of permeability, for four samples with very distinct pore sizes bracketing the entire range of pore size distributions

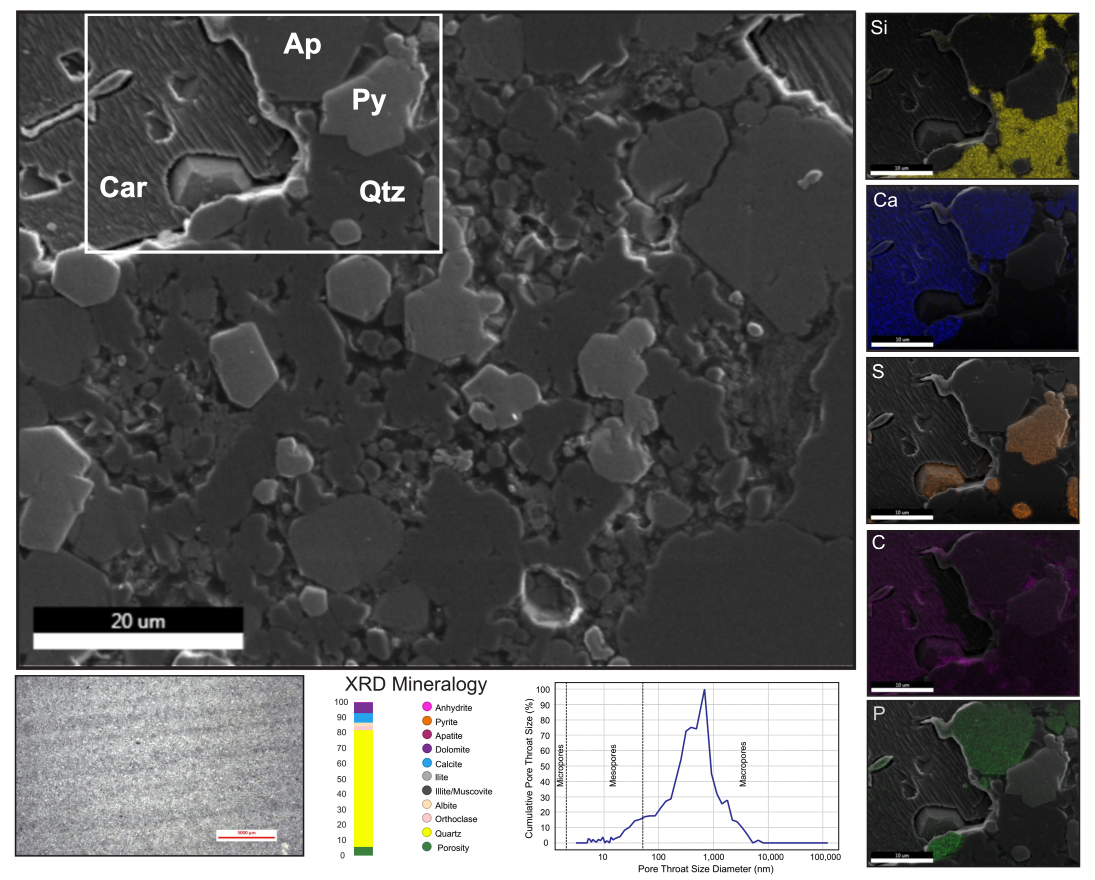

Figure 13 - SEM image of silica-rich siltstone sample TG13, with associated elemental maps used in the identification of mineral phases, as well as sample photograph, XRD mineralogy and incremental pore size distribution curve from mercury injection

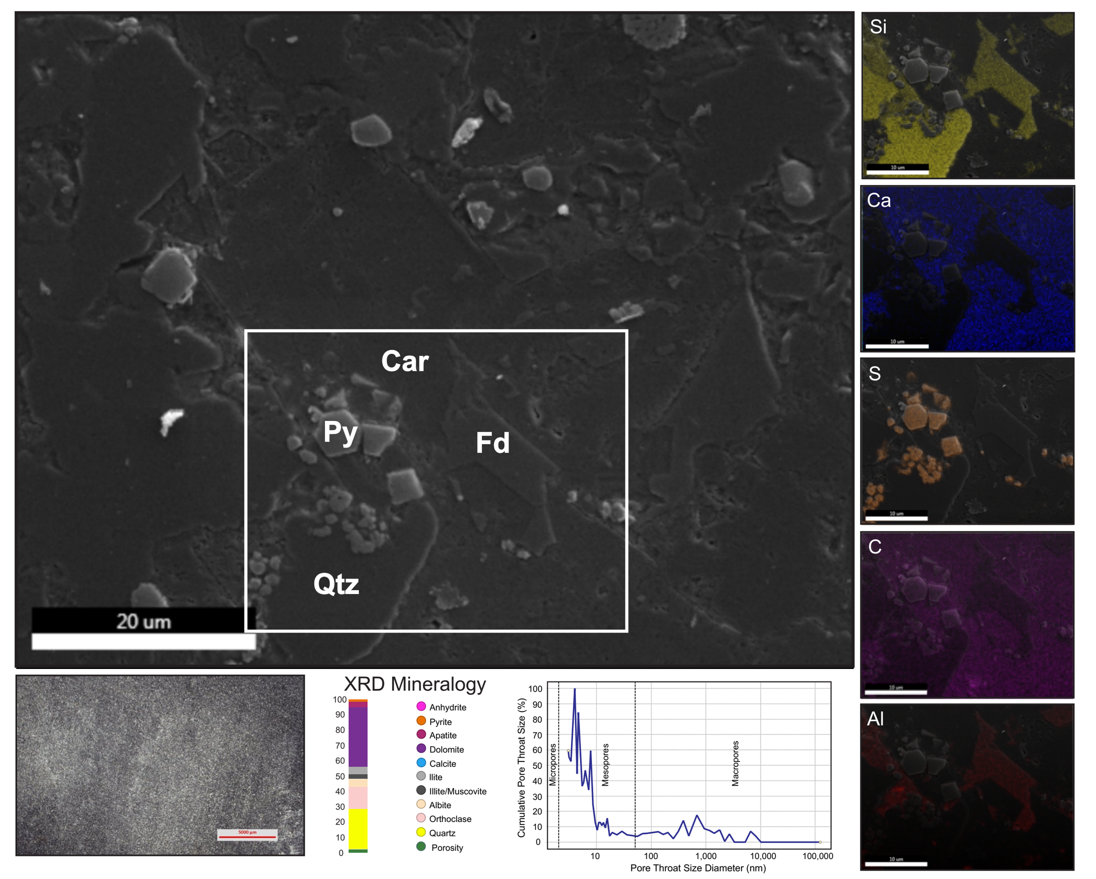

Figure 14 - SEM image of carbonate-rich mudstone sample HM1 with associated elemental maps used in the identification of mineral phases, as well as sample photograph, XRD mineralogy and incremental pore size distribution curve from mercury injection

Introduction

The Triassic Doig Formation of the Western Canada Sedimentary Basin is continuous across northeastern British Columbia and western Alberta. It historically had limited production from conventional reservoirs and was viewed as a source-rock for other conventional reservoirs in the basin. In the last five years, the Doig Formation has been recognised as an important unconventional reservoir for gas and natural gas liquids. Estimates of total gas in-place range from 40 to 200 Tcf (Walsh et al., 2006).

The Doig was deposited in the Middle Triassic, between the Anisian and Ladinian, and is part of the Daiber Group with the underlying Montney Formation.

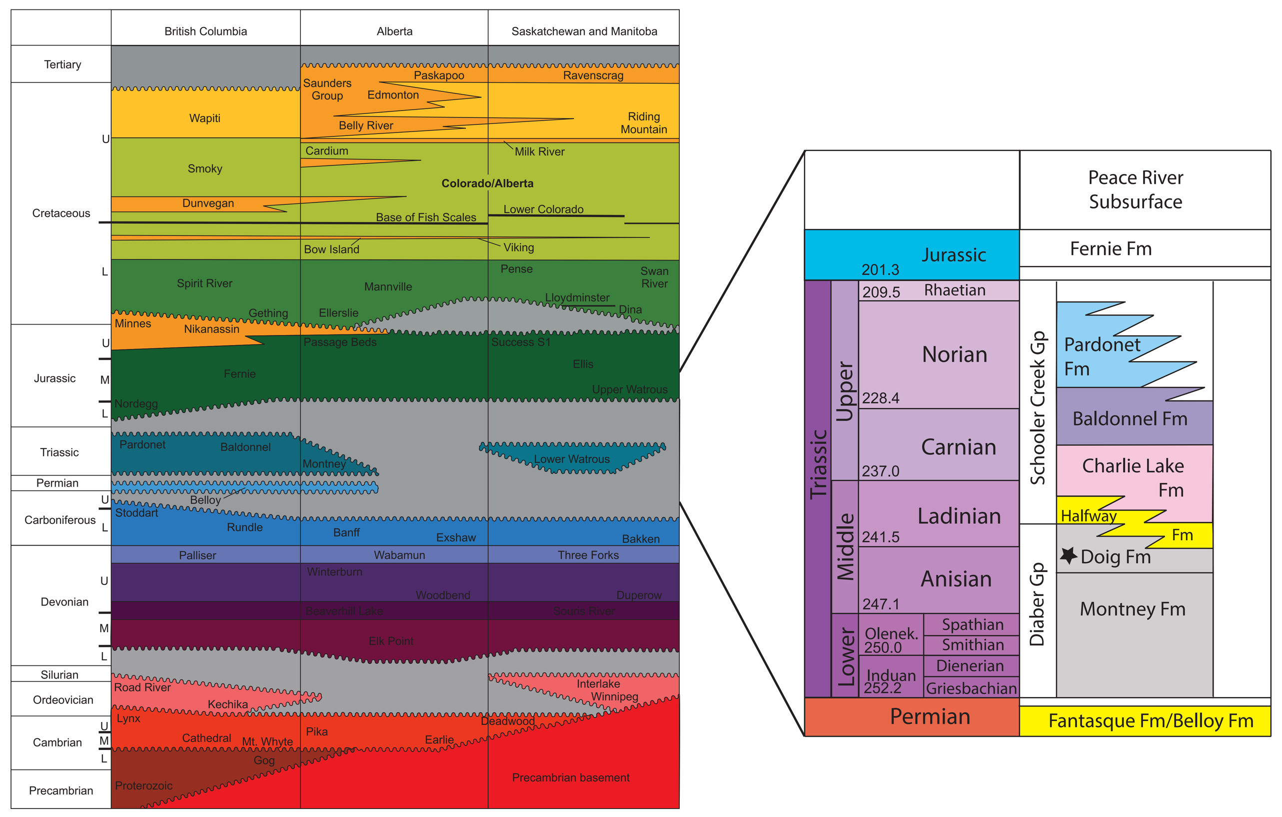

Figure 1 - Stratigraphic chart of the Western Canada Sedimentary Basin and expanded view of the Triassic (after Mossop and Shetsen, 1994; Golding et al., 2016)

The Triassic in the Western Canada Sedimentary Basin marks the transition from a carbonate-dominated intra-cratonic and passive margin that had persisted during the Paleozoic, to a siliciclastic-dominated relatively active embryonic foreland basin in the Triassic and Jurassic. The sedimentation of the Doig was influenced by the distribution of the underlying Devonian Leduc reef and the Mesozoic reactivation of the Mississippian Dawson Creek Graben Complex. The overall structural dip is southwest, where the Doig is the thickest and deepest, reaching 4,400 m of burial depth and 500 m in thickness.

The drifting of Pangaea into a subtropical and temperate climate midlatitudinal position, caused the westward facing margin of Pangaea to become very arid under the influence of trade winds, which also curtailed carbonate productivity. During the mid-Triassic, a sedimentary environment consisting of dominantly fine-grained siliciclastic marine shelves and ramps with extensive associated aeolian and evaporitic environments with low fluvial input occured.

The Doig was deposited under marine conditions from shoreface to offshore, and presents a wide variety of lithofacies, including very fine sandstones, siltstones, mudstones and bioclastic packstones.

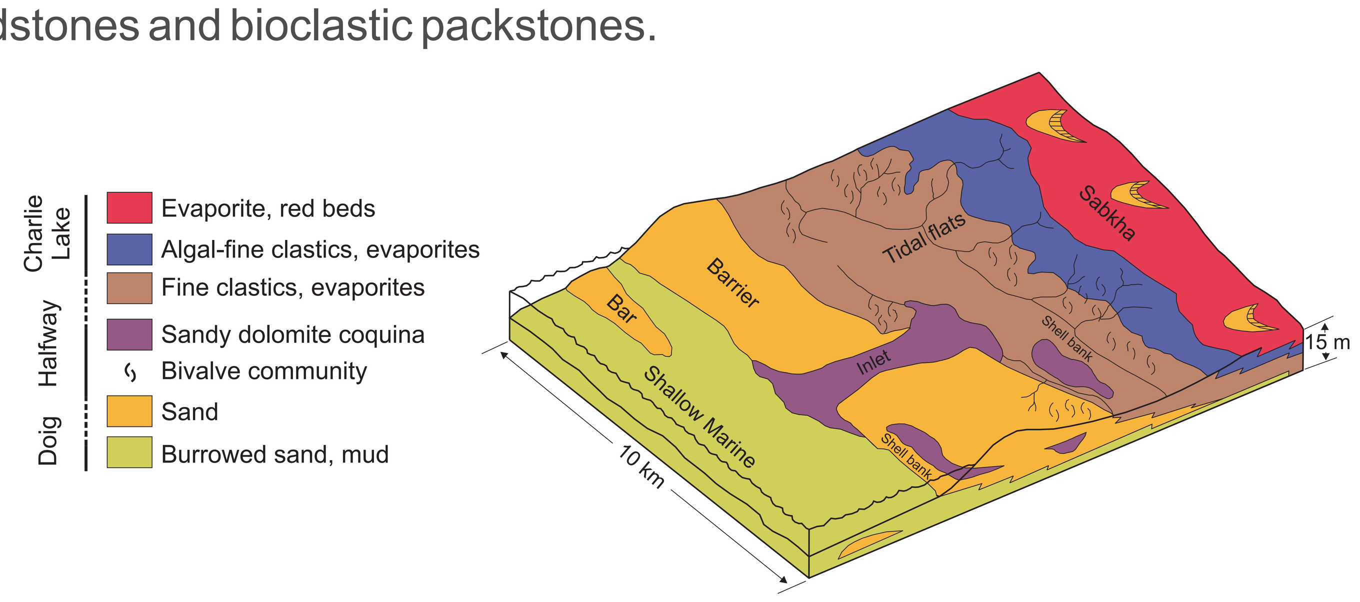

Figure 2 - Depositional environments of the Doig and associated formations (after Barclay and Leckie, 1986; Edwards et al., 1994)

The Doig is informally subdivided into three units. The basal unit, Doig A, is also known as the Doig Phosphate is an organic-rich radioactive mudstone with common phosphate granules and nodules. The intermediate Doig B is primarily composed of intercalated mudstones and siltstone. The upper Doig C is composed of relatively organic-lean siltstones and fine sandstones.

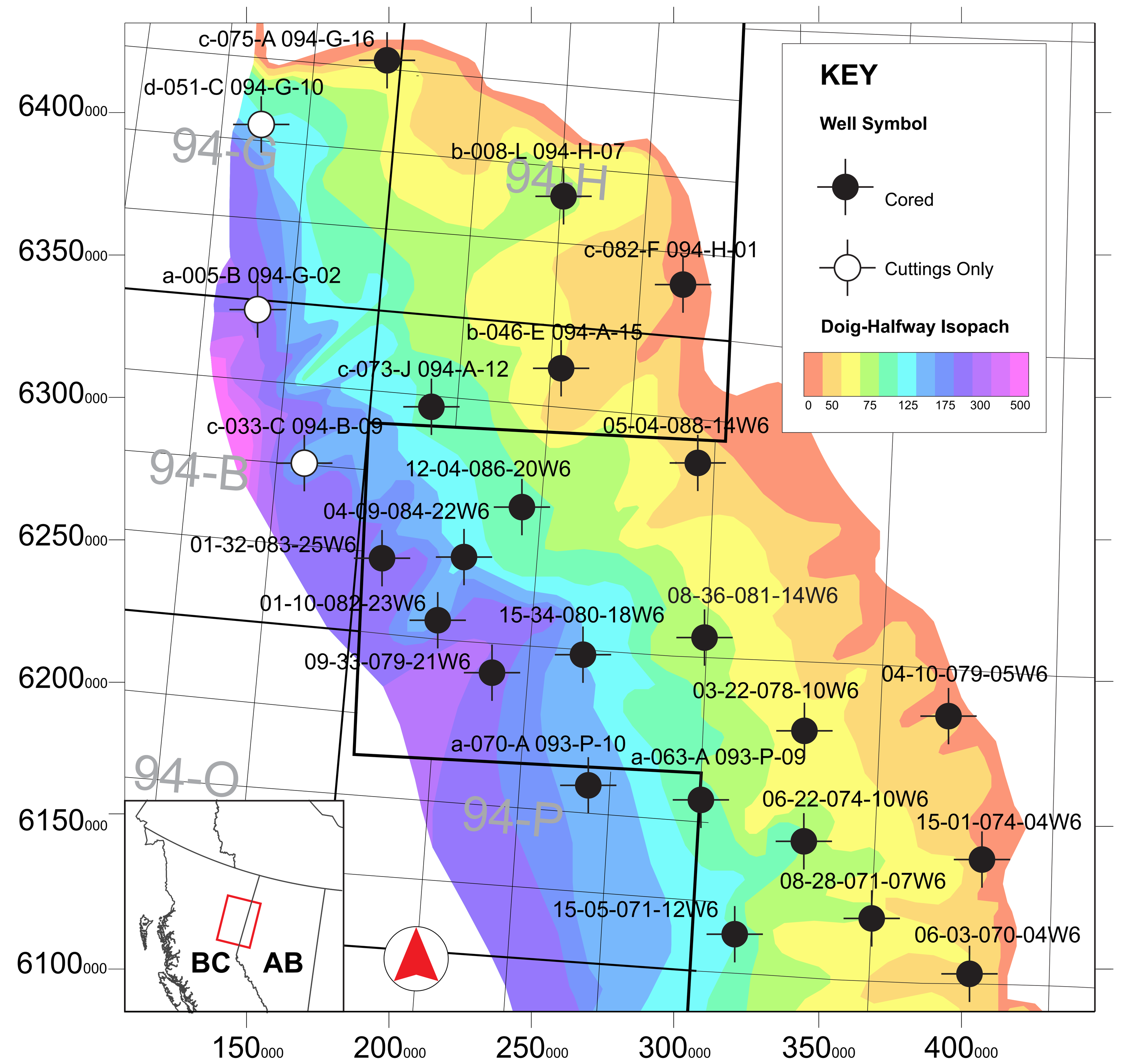

Figure 3 - Wells included in this study, overlain on isopach map of the Doig-Halfway interval (after Dixon, 1999)

The timing of hydrocarbon generation and migration is poorly constrained, but hydrocarbon generation is thought to have started in Late Jurassic, reaching maximum transformation rate during Early Paleogene, before the last major erosion. Hydrocarbon migration from the Doig is thought to have occurred as late as Early Cretaceous. Studies on petrophysics and organic geochemistry of the Doig are sparse and limited in scope. The geological control on the petrophysical and organic geochemical properties of the Doig and their spatial and stratigraphic distribution is also currently poorly understood.

Objectives

In this poster we present preliminary results on the petrophysical and organic geochemical properties of the Doig Formation, which are part of an ongoing petroleum system analysis of the Doig. The project objectives are:

- Understand the spatial and stratigraphic variability in the petrophysical properties of the Doig Formation;
- Determine how lithofacies and mineralogy affect the pore size distribution and permeability;
- Assess the potential for gas and natural gas liquids over the entire extent of the Doig by determining the organic richness, maturity range and timing of hydrocarbon generation and migration.

Methods

This study is based on core and cutting samples from 25 wells from British Columbia and adjacent area in Alberta, distributed along the entire spatial extent of the Doig Formation. Samples were analyzed to determine mineralogy, porosity, pore-size distribution (PSD), permeability, total organic carbon (TOC), temperature of maximum hydrocarbon generation (Tmax), and kerogen type.

Porosity was determined on all core samples by a combination of helium pycnometry skeletal density and mercury buoyancy bulk volume measurements. Another source of porosity data, as well as pore throat size distribution is mercury injection porosimetry. Mineralogy was determined by X ray diffraction (XRD). Permeability was determined by pulse-decay gas permeameter, and Tmax, TOC and kerogen type were determined through Rock-Eval type pyrolysis on cutting samples in order to achieve a higher data density and continuous profiles. The pore structure was investigated with the use of scanning electron microscope (SEM) images.

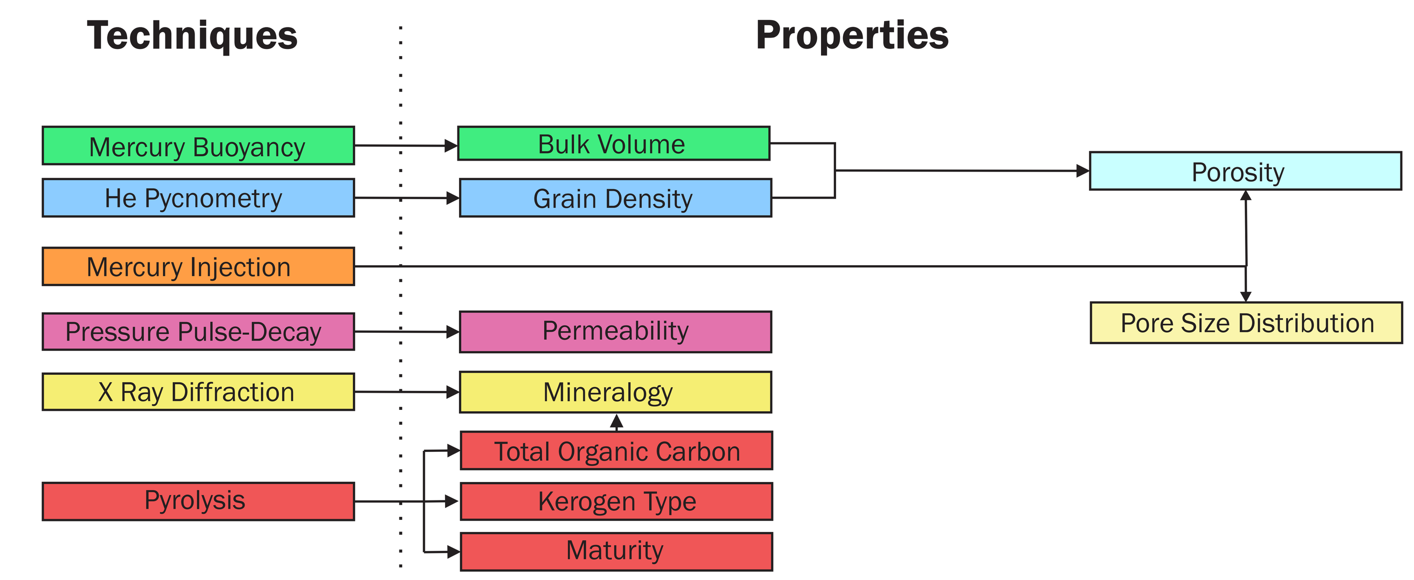

Figure 4 - Flow chart of the methods used in this study in order to derive petrophysical and organic geochemical properties

The gas expansion pycnometry was measured four times before drying and four after drying, on crushed rock of 20 to 35 mesh size; the equilibrium time was set to 300 seconds. The unstressed porosity is obtained by mass balance calculation once the density of the solid framework (grain density) and of the bulk rock (bulk density) are established, by assuming a fluid density of air. Mercury intrusion was done on crushed rock of 4 to 8 mesh, cleaned with solvent and oven-dried. The intruded volumes were corrected for closure and compressibility effects. Pore throat radius is calculated through the Washburn equation with mercury-air interfacial tension and contact angles and assuming cylindrical capillary tube pore radius geometry.

Mineralogy was obtained by XRD using powdered samples smear-mounted on glass slides. Permeability was determined by pulse-decay gas permeameter using He at effective stresses between 1,000 and 5,500 psi, by varying the net confining stress while keeping the pore pressure constant.

Pyrolysis was done using a Rock-Eval type instrument on 70 mg of powdered sample, at a temperature rate of 25 °C per minute until 650 °C, followed by a temperature decrease and oxidation stage at 730 °C.

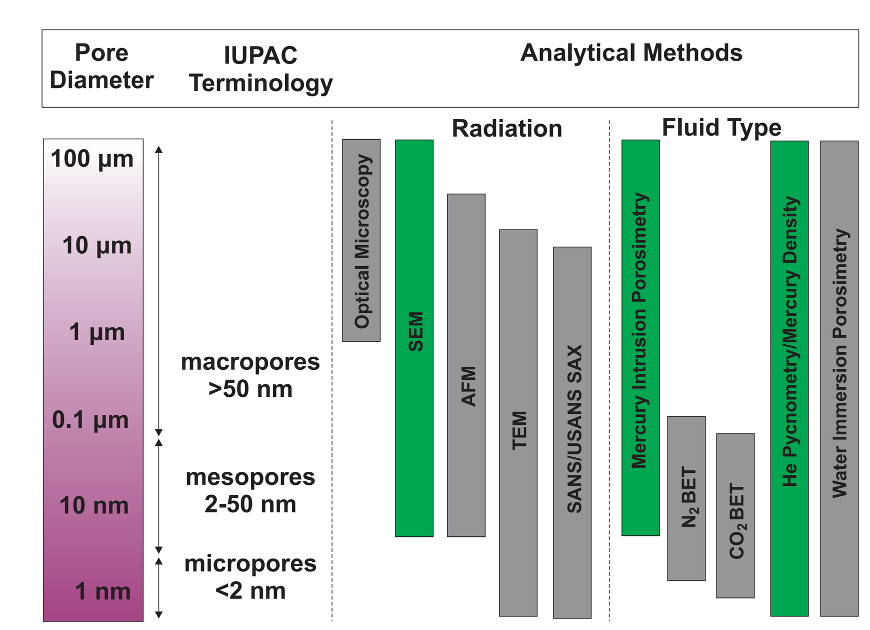

Figure 5 - Analytical methods commonly used for determination of porosity and their ranges of pore size investigation, with methods used in this study highlighted in green

a place of mind

Organic Geochemistry

The Doig samples analyzed show a wide range of TOC and degree of thermal maturity. The average TOC is 1.9% and the maximum is 6.4%, with the 80% confidence interval distributed between 0.8% and 3.3%. The highest TOC values are observed in the upper Doig A member.

Most samples are mature and within the oil window. Less than 5% of the samples were overmature, with Tmax values as high as 490 °C. A few samples were immature, albeit most of which are unreliable due to poor quality Tmax peak.

There is a wide range of Tmax values for any given present-day depth across the basin, suggesting the paleo-depth of burial had a strong influence on the present-day maturity. Although, shallower wells in the eastern portion of the basin tend to show lower maturities, second and third order controls impose a more complex pattern. Especially in the thicker successions of the westernmost wells, a wide range of maturity is observed on a single well.

Combined use of pseudo van Krevelen and Tmax vs. HI plots suggests that the organic matter is primarily of kerogen type III, with minor contribution from type II-III.

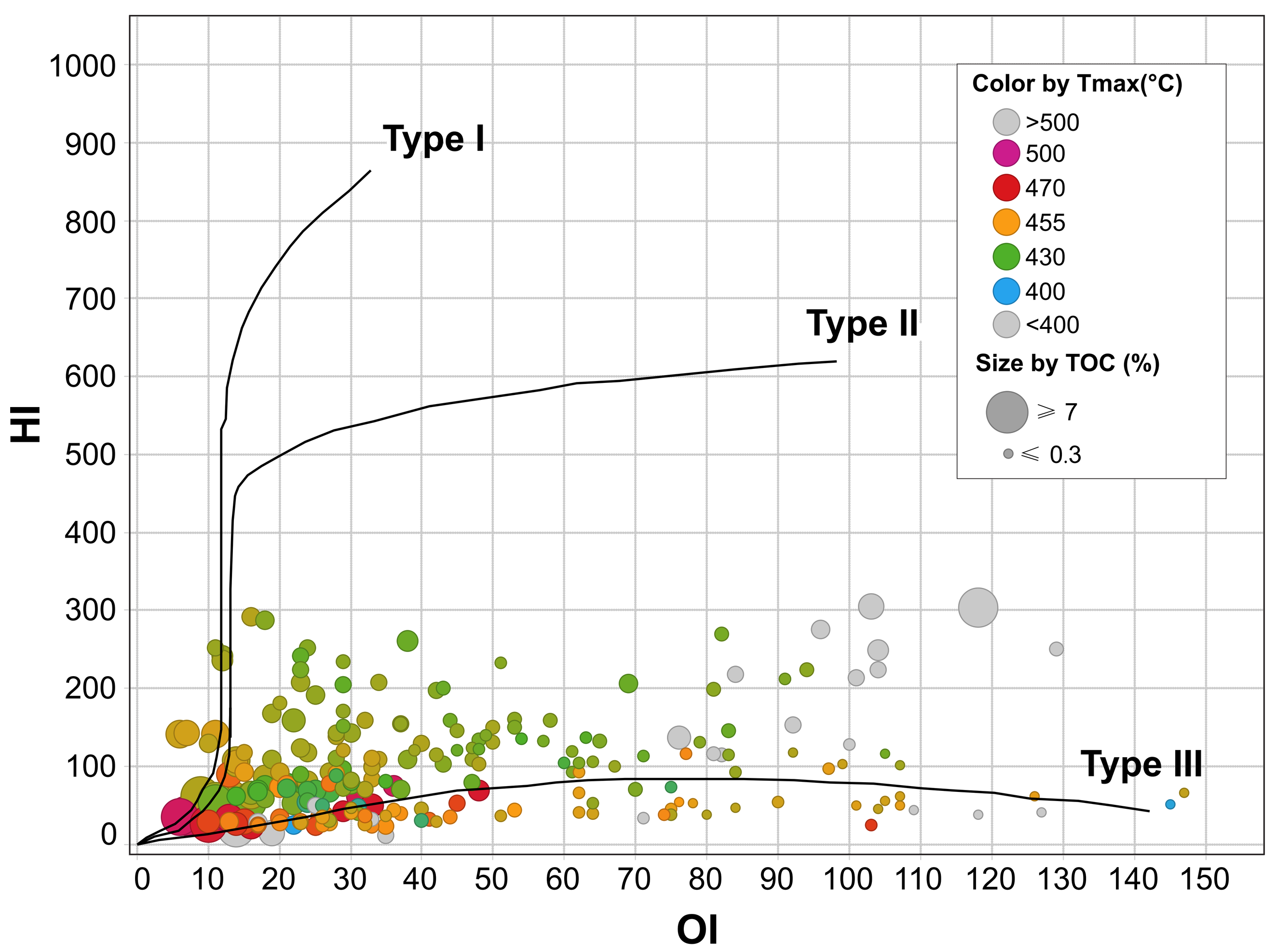

Figure 15 - Pseudo van Krevelen plot showing the thermal evolution path of the two types of kerogen present

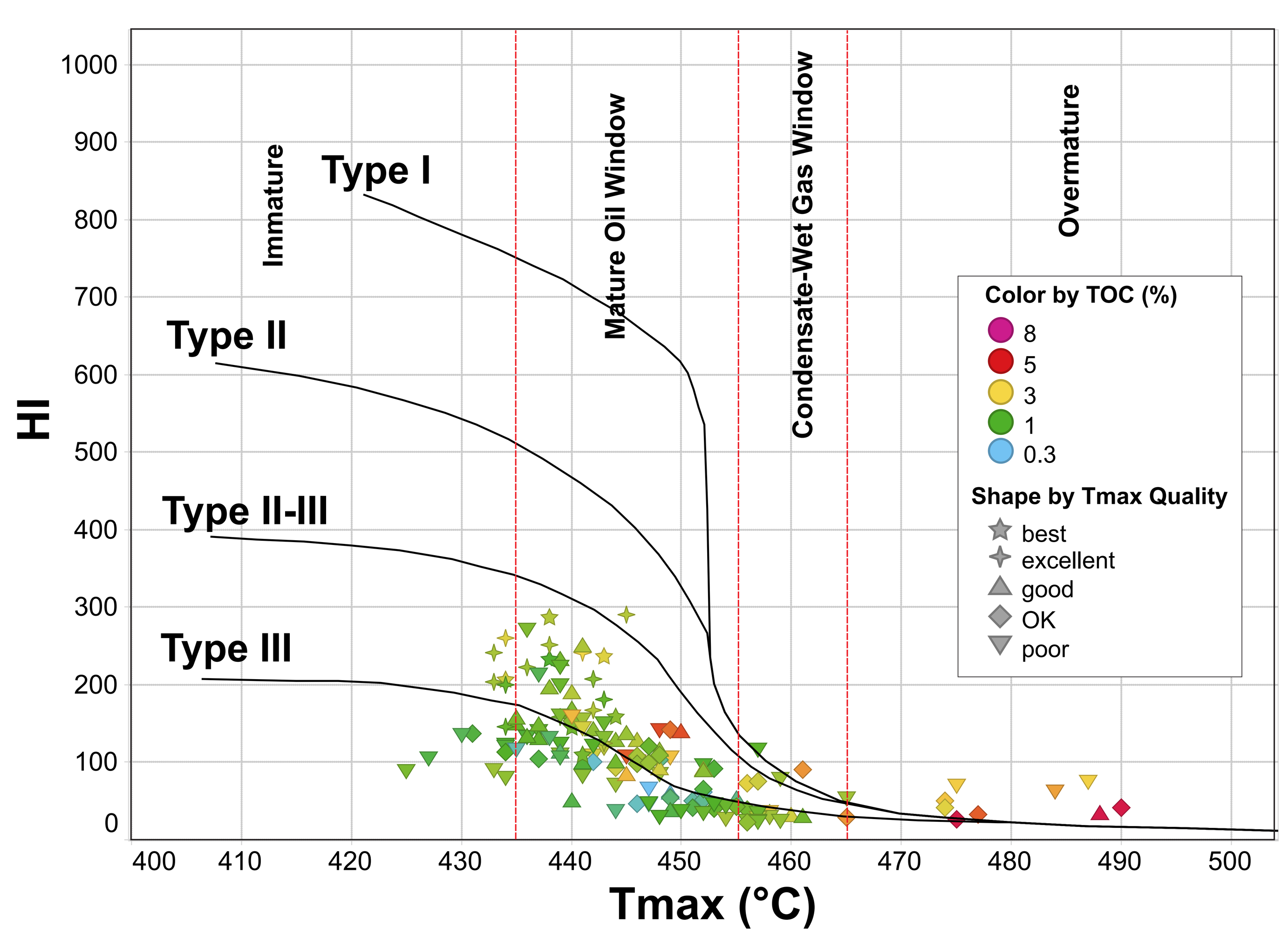

Figure 16 - Tmax vs. HI plot showing the kerogen type and thermal degradation path of kerogen from the immature to overmature windows

Conclusions

Mineralogy

• The Doig siltstones and mudstones are primarily composed of silicates and carbonate, with only minor amounts of clay; the main clay mineral is illite, with subordinate amounts of chlorite.

• The Doig C is the most homogenous member being composed primarily of clay-free quartz-rich massive siltstones and cross-bedded fine sandstones.

• Doig B is the most variable member in terms of facies and mineralogy, ranging from carbonate-rich massive, bioturbated or bioclastic mudstones to silica-rich wavy laminated silstones with sparse carbonate laminae.

•The Doig A mudstones have the highest amount of clay, and common occurrence of pyrite, but show a highly variable proportion between silica and carbonate.

Porosity, Pore Size and Permeability

• Porosity is highly variable, ranging from 0.6% to 16.4%.

• Porosity is partly controlled by clay and calcite, probably in the form of carbonate mud; the higher porosity samples are poor in clay and calcite and rich in silicates.

• Mercury injection porosities are consistently lower than the helium pycnometry ones, due to pore size accessibility limitations, but are demonstrated to be reliable if properly corrected;

• Matrix permeability spans four orders of magnitude, from 7E-02 mD to 3.5E-05 mD at effective stresses of 2,500 psi and show a good correlation with porosity; the mineralogy plays a key control in determining pore volume compressibility; the quartz-rich siltstones do not have stress dependent permeability.

• The pore size is also a key controlling factor in determining the permeability, with the mostly meso and microporous relatively clay-rich mudstones showing the lowest permeability values; the silicate-rich siltstones, which have median pore throat size two orders of magnitude larger, well in the macroporosity region, exhibit the highest permeabilities.

Organic Geochemistry

• The average TOC is 1.9%, with a minimum of 0.3% and maximum of 6.4%.

• The primary kerogen is of type III, with secondary contribution from type II-III.

Future and Ongoing Work

• Low-pressure gas adsorption to characterize the distribution, and FIB-SEM to image the structure of the microporosity.

• Additional mercury injection and pulse-decay permeability measurements for refining the correlation between pore throat size and permeability.

.

• Additional X ray diffraction and triaxial tests in order to derive correlation between mineralogy, ultrasonic velocity and geomechanical properties.

• Petroleum system analysis of the Doig with a basin model calibrated to source-rock and reservoir properties, as well as present-day thermal maturity indices.

References

Barclay, J.E. & Leckie, D.A., 1986. Tidal inlet reservoirs of the Triassic Halfway Formation, Wembley Region, Alberta. In N. C. Drees, Meijer, ed. Core Conference. Calgary: Canadian Society of Petroleum Geologists, pp. 4.1–4.6.

Edwards, D.E. et al., 1994. Triassic Strata of the Western Canada Sedimentary Basin. In G. D. Mossop & I. Shetsen, eds. Geological Atlas of the Western Canada Sedimentary Basin. Calgary: Canadian Society of Petroleum Geologists & Alberta Research Council, pp. 257–275.

Dixon, J. 1999. Isopach maps of some Triassic units in the Western Canada Sedimentary Basin. Geological Survey of Canada, Open File 3758.

Gamero-Diaz, H; Miller, C. and Lewis, R., 2012, Core: A classification scheme for organic mudstones based on bulk mineralogy, Search and Discovery article # 40951.

Golding, M. L., Mortensen, J. K., Ferri, F., Zonneveld, J-P, Orchard, M., 2016. Determining the provenance of Triassic sedimentary rocks in northeastern British Columbia and western Alberta using detrital zircon geochronology, with implications for regional tectonics. Canadian Journal of Earth Sciences, 53 (December 2015), pp.140–155.

Mossop, G.D. and Shetsen, I. 1994. Introduction In: Geological Atlas of the Western Canada Sedimentary Basin. Mossop, G.D. and Shetsen (eds.). Canadian Society of Petroleum Geologists and Alberta Research Council, Calgary, p. 1–11.

Walsh, W., Adams, C., Kerr, B., Korol, J. 2006: Regional “shale gas” potential of the Triassic Doig and Montney formations, northeastern British Columbia; in BC Ministry of Energy, Mines and Petroleum, Resource Development and Geoscience Branch, Petroleum Geology Open File 2006-02, 2006-02, 19 p.

Acknowledgements

The authors would like to acknowledge the financial support from Geoscience BC, Trican Geological Solutions Ltd., EnCana Corporation, Husky Energy Inc., Chevron Canada Limited, Canadian Natural Resources Limited, Geologic Systems Ltd., and Natural Sciences and Engineering Research Council of Canada; as well as Trican's staff for the generous lending of instruments and valuable expertise, especially Brent Nassichuk, Cory Twemlow, Nik Minions and Sam Tu.

We are also thankful for the assistance of Tenley Horsman, Chris Moll and Rhys O'Connor in sample preparation and analysis. Lastly, we acknowledge BC Oil & Gas Commission, Alberta Energy Regulators, Canadian Natural Resources Limited, ConocoPhillips Canada, Husky Energy Inc, TAQA North Inc., and Tidewater Midstream and Infrastructure Ltd. for providing the samples used in this research.